INTERNATIONAL SOCIETY FOR
SOIL MECHANICS AND
GEOTECHNICAL ENGINEERING

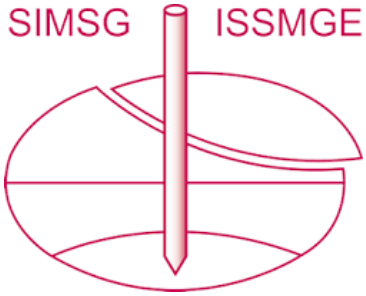


*This paper was downloaded from the Online Library of the International Society for Soil Mechanics and Geotechnical Engineering (ISSMGE). The library is available here:*

*https://www.issmge.org/publications/online-library*

*This is an open-access database that archives thousands of papers published under the Auspices of the ISSMGE and maintained by the Innovation and Development Committee of ISSMGE.*

*The paper was published in the proceedings of the 7th International Conference on Earthquake Geotechnical Engineering and was edited by Francesco Silvestri, Nicola Moraci and Susanna Antonielli. The conference was held in Rome, Italy, 17 – 20 June 2019.*

*Earthquake Geotechnical Engineering for Protection and Development of Environment and Constructions – Silvestri & Moraci (Eds)*
*© 2019 Associazione Geotecnica Italiana, Rome, Italy, ISBN 978-0-367-14328-2*

# Ground motion amplifications due to topographic effects during the 2017 Pohang earthquake, South Korea

S. Kang, B. Kim & S. Bae
*Ulsan National Institute of Science and Technology, Ulsan, South Korea*

K. Kim
*Heesong Geotek, Gyeonggi, South Korea*

H. Cho
*Korea Institute of Geoscience and Mineral Sources, Daejeon, South Korea*

ABSTRACT: An M5.4 (moment magnitude) earthquake struck the Pohang, South Korea on November 15, 2017 at 14:29:31 local time (05:29:31 UTC). The Pohang city experienced various damages attributed to a shallow focal depth (3-7 km). We observed numerous damages at Gokgang-ri located 3.5 km east of the main shock epicenter (36.109°N and 129.366°E). The northern part of Gokgang-ri, located on a slope facing to the epicenter or on a plateau after slope, suffered severe damages. However, the southern part on a slope facing to the opposite direction experienced only few damages. We installed four temporary seismic stations in Gokgang-ri, and measured ground motions from several aftershocks (M1.8-M3.8). Amplification factors recorded on the northern part are larger than those on the southern part. Given the similar geological/soil conditions between two parts in Gokgang-ri, we conclude that the different extents of damages are resulted from ground motions amplified due to surface topographic irregularities.

## 1 INTRODUCTION

An earthquake with a moment magnitude (M) of 5.4 occurred in Pohang city, North Gyeongsang Province on November 15, 2017 at 14:29:31 local time (05:29:31 UTC). The epicenter of main shock is located in Namsong-ri, Heunghae-eup, Buk-gu, Pohang city, North Gyeongsang Province at 36.109°N and 129.366°E with a focal depth of 3 to 7 km (Korea Meteorological Administration 2017). This earthquake is the second largest instrumented earthquake in South Korea, following the 2016 Gyeongju earthquake (M5.5) (National Earthquake Comprehensive Information System (NECIS) 2018). Although the magnitude of the Pohang earthquake (M5.4) was smaller than that of the Gyeongju earthquake (M5.5), the Pohang earthquake caused various structural damages (Figure 1) and geotechnical deformations (Figure 2) which are more severe and prevalent than the damages caused by the Gyeongju earthquake.

Figure 1. Examples of structural damages caused by the 2017 Pohang earthquake.


Figure 2. Examples of ground deformations caused by the 2017 Pohang earthquake.

The severe damages caused by the Pohang earthquake with the moderate magnitude might be attributed to the shallow focal depth of approximately 4 km and effects of ground motion amplification affected by a depth to bedrock in the Pohang basin, approximately 500 m (Kang et al. 2019). These environments might be vulnerable to damages caused by earthquakes.

We observed unusual damage patterns in a village named Gokgang-ri composed of northern and southern parts during our field investigates. Damages were severe in the northern part. However, only few minor damages occurred in the southern part. The northern part is on slopes facing to the main shock epicenter, on plateaus after slopes, or on ridges (upslopes from a direction of the epicenter), but the southern part is on slopes facing to the opposite directions (downslope from a direction of the epicenter). We supposed that different topographic characteristics caused the different damage patterns between the two parts.

Previous studies in relation to topographic effects-induced ground motion amplifications have been conducted through a variety of approaches: (1) field observations or instrument records (e.g., Davis & West 1973, Hough et al. 2010, Wood & Cox 2016); (2) analytical solutions (e.g., Aki & Larner 1970, Savage 2004); (3) laboratory tests (e.g., Kovacs et al. 1971, Stamatopoulos et al. 2007); and (4) numerical methods (e.g., Ashford & Sitar 1997, Assimaki et al. 2005, Rai et al. 2016). Numerous past studies have focused on the topographic amplification at ridge crests, cliffs with steep slopes and hill tops and the de-amplification at canyons or hill toes based on various topographic geometries (e.g., slope angle, slope height, width of topographic feature, and direction of slope), characteristics of incident wave (e.g., direction of wave propagation, wave type and angle of incidence), reflection of seismic waves due to topographic surface irregularity, and effects of surface waves.

The main purpose of this study is to investigate effects of topographic features on ground motion amplifications. We recorded several aftershock ground motions (M1.6-M4.6) at four temporary seismic stations that we installed in Gokgang-ri. We also measured shear-wave velocities around the study area to understand near-surface soil characteristics by using multichannel analysis of surface waves (MASW) and downhole tests.

## 2 STUDY AREA

The study area, Gokgang-ri, is approximately 3.5 km away from the main shock epicenter to the East. Figure 3 shows a location of the study area and geology information around the northern Pohang city. Outcropping lithology near the study area is composed of Cretaceous system, Tertiary system and Quaternary Alluvium (Geological Survey of Korea 1964). More

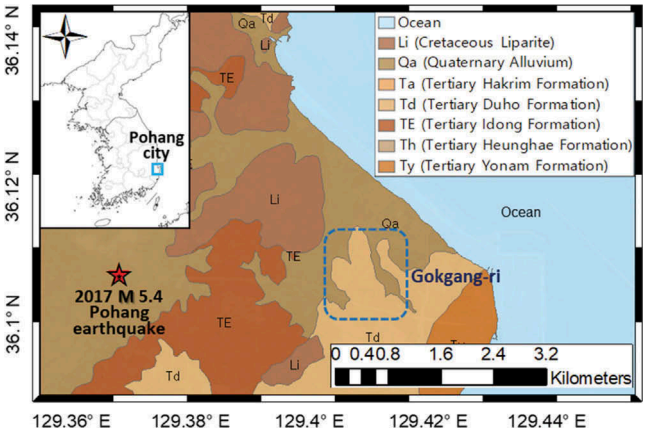


Figure 3. Geological map around Gokgang-ri (modified from Geological Survey of Korea, 1964).

portion of the study area is covered by Tertiary Duho Formation as shown in Figure 3. In general, near surface grounds of the Pohang area are covered by soft grounds including sedimentary and fill soils (Hwang et al. 1995).

We carefully inspected damages of all 65 buildings in the study area and classified the damages into five grades depending on the criteria shown in Figure 4. Among the total 65 buildings, 12, 16, 21, 11 and 5 houses were classified as Damage Grade from 1 to 5, respectively. While 36 buildings among 54 buildings (approximately 67 percent) in the northern part of the study area suffered severe damages (Damage Grades 3-5), buildings in the southern part experienced only minor damages (Damage Grades 1-2) as shown in Figure 5a.

Considering the damage patterns of the two parts despite similar geological conditions and similar directions and distances from the main shock epicenter, it is possible that topographic features caused strong ground motion amplifications on the north part. The northern part is on slopes facing to the main shock epicenter, on plateaus after slopes, or on ridges (upslopes from a direction of the epicenter), but the southern part is on slopes facing to the opposite directions (downslope from a direction of the epicenter). We determined locations to install four temporary seismic stations (GOK1 to GOK4) considering topographic features and the Damage Grades to measure aftershock ground motions. The house with a short distance from GOK1 on a slope facing to the epicenter in the northern part suffered severe damages (Damage Grade 5); the house near GOK2 on a slope facing to the opposite direction in the


Figure 4. Examples of the criteria used to classify Damage Grade 2 through 5. If no damage is observed, Damage Grade is classified as 1.

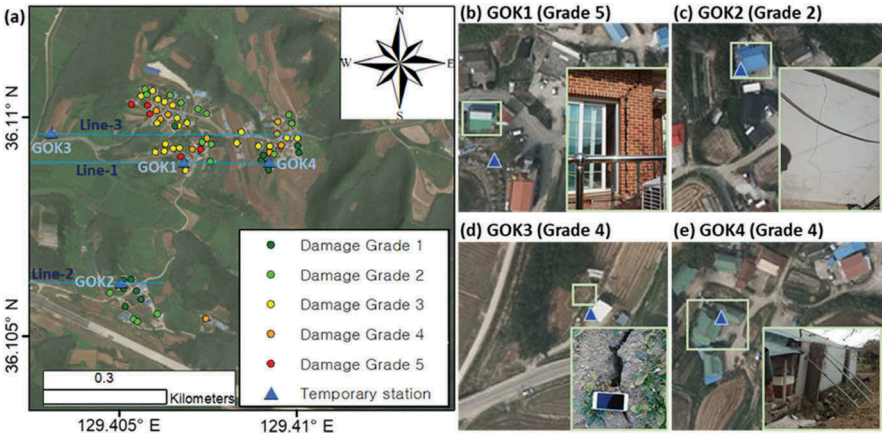


Figure 5. (a) Locations of buildings in Gokgang-ri with the corresponding Damage Grades and four temporary stations, GOK1 through GOK4. Three straight lines in the West-East direction, Line-1 through Line-3, were utilized to analyze topographical profiles shown in Figure 6. (b) through (e) Locations of the four stations and damages in the vicinity.

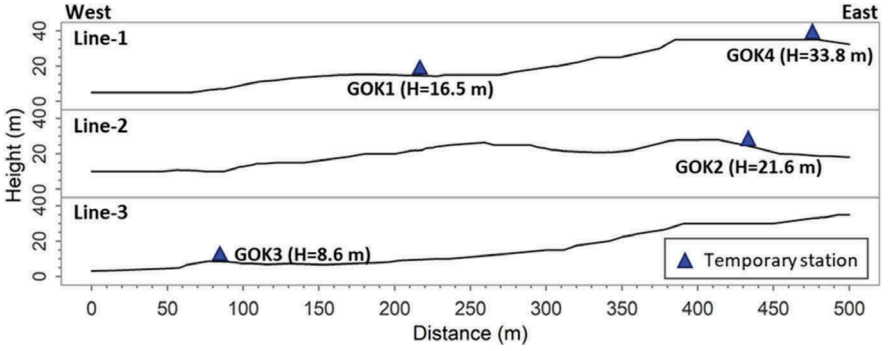


Figure 6. Topographical profiles on the three straight lines in the West-East direction shown in Figure 5a and Locations of the four seismic stations (GOK1-GOK4) on the profiles. The topographic profiles were computed from a 1:5000 digital map.

southern part suffered several small cracks (Damage Grade 2); GOK3 was installed on the crest of the very gentle slope most similar to a reference site condition because we could not find a reference site in the study area (it is difficult to find rock outcrop in free fields in Korea as reference sites); and the building near GOK4 on a plateau in the northern part suffered a large crack between exterior wall and the building (Damage Grade 4) (Figures 5b-e and, 6). The paddy next to GOK3 suffered moderate ground cracks (Damage Grade 4). All the stations are on the sites covered by Tertiary Duho Formation.

## 3 $V_S$ PROFILES NEAR STATIONS

We conducted field tests, such as downhole test and multi-channel analysis of surface waves (MASW) method, to investigate shear-wave velocity ($V_S$) near the temporary seismic stations that has an important effect upon ground motion amplifications. Figure 7 shows the $V_S$ profiles resulted from downhole tests conducted at two sites near GOK1 and GOK2, as well as the profiles obtained through MASW conducted at four sites near GOK1 through GOK4. The $V_S$ profile near GOK1 from MASW is approximately 200 m/s smaller than that from downhole test at

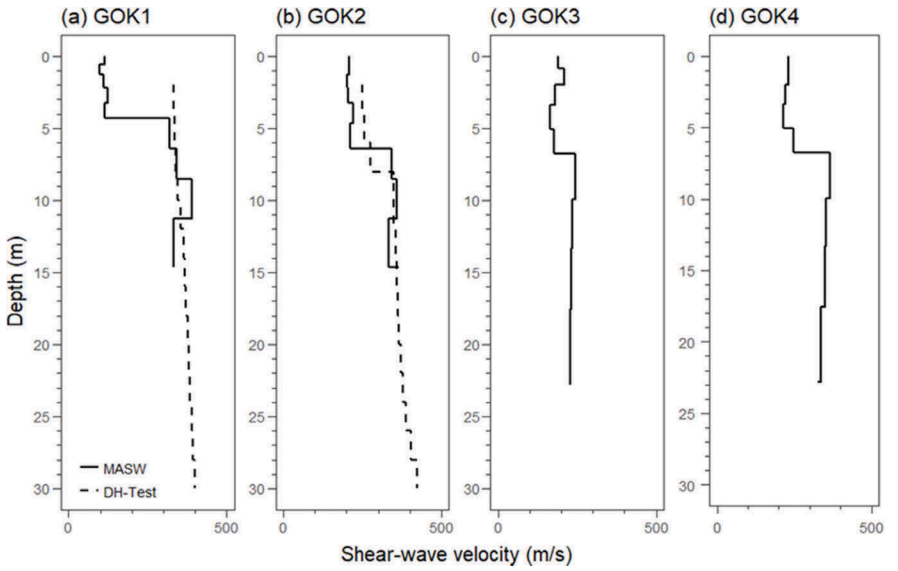


Figure 7. Shear-wave velocity profiles resulted from downhole (DH) tests at sites near GOK1 and GOK2 and from the MASW method at sites near GOK1 to GOK4: (a) to (d) near GOK1 to GOK4.

shallow depths within 5 m because the test site for MASW (near GOK1) being used as an orchard is covered by soft soils at shallow depths while soils at shallow depths around the site for downhole test (near GOK1) are well compacted. The $V_S$ profiles from the both methods are similar near GOK1 at depths deeper than 5 m, and the profiles obtained from MASW and downhole test near GOK2 show similar values as shown in Figure 7a, b. The $V_S$ profiles near GOK1 through GOK4 generally show small values in a range of 200-400 m/s.

## 4 AFTERSHOCK INFORMATION

We measured four aftershock ground motions with a sampling frequency of 200 Hz in EW (East-West), NS (North-South), and UD (Up-Down) directions at the four temporary seismic stations (GOK1 through GOK4) installed in the study area. Information of the aftershocks recorded in this study (e.g., moment magnitude (M), occurrence time, focal depth, epicentral distance to the study area, and incidence angle of seismic wave estimated using the focal depth and the epicentral distance) are in Table 1. Figure 8 show epicenters of the main shock and the four aftershocks and locations of the four seismic stations. Direction from an epicenter of Aftershock 3 to the study area deviate slightly from the East-West direction. However, topographic profiles near the study area along the wave paths from the epicenter of the Aftershock 3 are similar to the topographic profiles in the E-W direction (as shown in Figure 6).

Table 1. Information of the aftershocks measured in this study (NECIS 2018).

| Aftershock no. | Magnitude (M) | Occurrence date (local time) | Focal depth (km) | Epicentral distance to Gokgang-ri (km) |
|---|---|---|---|---|
| Aftershock 1 | 3.8 | Dec 25, 2017 16:19:23 | 5.6 | 3.8 |
| Aftershock 2 | 1.8 | Dec 25, 2017 16:32:04 | 8.0 | 3.9 |
| Aftershock 3 | 2.0 | Dec 26, 2017 04:05:47 | 6.0 | 4.3 |
| Aftershock 4 | 2.9 | Dec 27, 2017 19:27:46 | 8.0 | 3.8 |

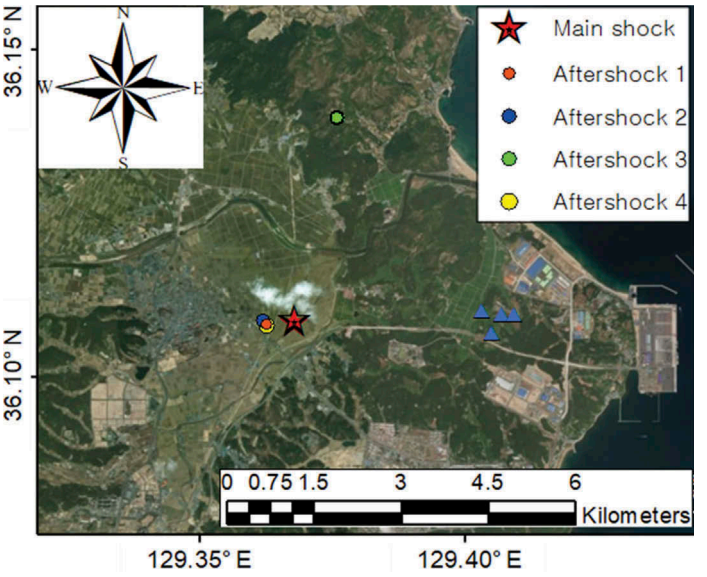


Figure 8. Locations of epicenters of the main shock and the four aftershocks and the four temporary seismic stations (triangles).

## 5 COMPARISON OF FOURIER AMPLITUDES

We recorded ground motions in the EW, NS, and UD directions at the four stations during the four aftershocks listed in Table 1. Smoothed Fourier amplitude spectrum were computed in the EW, NS, and UD directions using the four aftershock ground motions as shown in Figure 9. We used DEEPSOIL v6.1 developed by Hashash et al. (2016) to compute smoothed Fourier amplitude spectrum to evaluate frequency content of the aftershock ground motions. Peak Fourier amplitudes exist at frequencies in the range of 3-20 Hz which are approximate to natural frequencies of most damaged buildings (1-2-storey) in the study area.

In general, Fourier amplitudes at frequencies of 1-20 Hz at GOK1, GOK3 and GOK4 on the slopes facing to epicenters or on the plateaus are 1-3 times larger than those at GOK2 on the slope facing to the opposite direction, which is consistent with the damage pattern observed in the study area. These ground motion amplifications result from topographic effects considering the similar epicentral distances, $V_S$ profiles, and geological conditions near the four stations. Peak amplifications of all the ground motions at GOK1 and GOK4 (in the northern district) relative to GOK2 (in the southern district) mainly occur at frequencies of 1-20 Hz with spectral ratios ranging from approximately 2 to 5. It is possible that the strong ground motion amplifications at the northern district at frequencies of 1-20 Hz could result in severe damages in the 1-to-2-story houses given the similar range of natural frequencies of the houses.

According to the previous studies (e.g., Boore 1972, Davis & West 1973, Wood & Cox 2016), relatively steep topographic feature has effects on ground motion amplifications. In addition, many numerical simulations have focused on topographic amplifications on steep slopes (i.e., slope angles  30°) using input motions with relatively small incidence angles (the angle of incident wave propagation with respect to the vertical) less than 30° (e.g., Ashford & Sitar 1997, Assimaki et al. 2005, Rai et al. 2016, Asimaki & Mohammadi 2018). On the other hand, the slopes of the study sites where the houses were severely damaged (near GOK1 and GOK4) are gentle with gradients smaller than 8°. Incidence angles of the incident waves range from 24.6° to 59.5° (estimated by using focal depths and epicentral distances presented in Table 1). These large incidence angles possibly increase the chances of generating surface waves (i.e., Rayleigh wave and Love wave) according to Bowden and Tsai (2017) and Tsai et al. (2017). Strong Rayleigh waves can be generated by incident SV waves at the foot of the

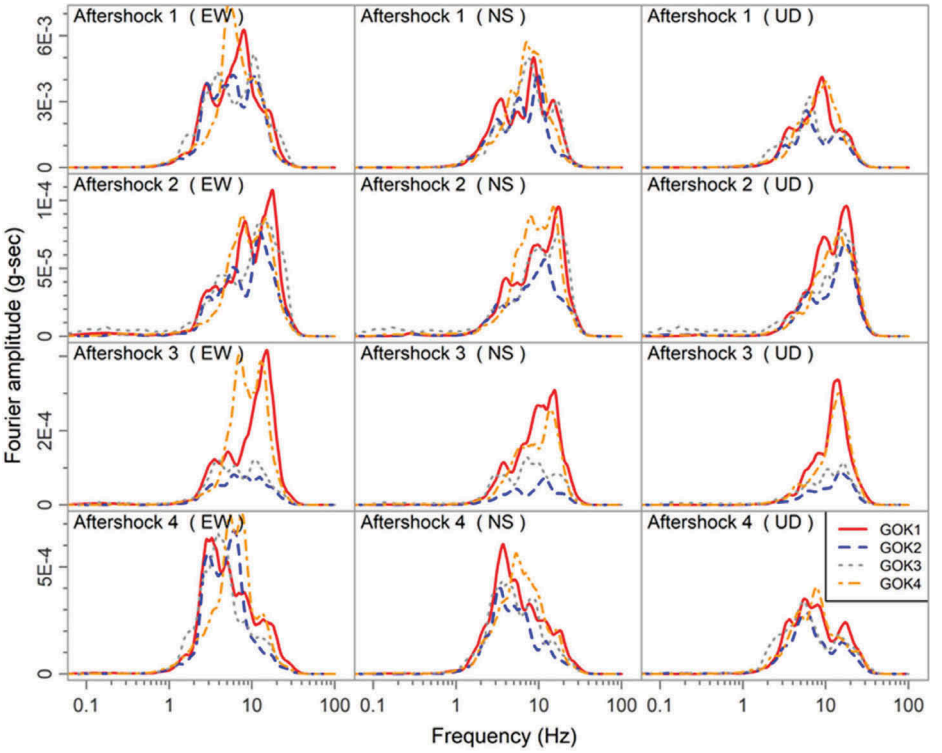


Figure 9. Acceleration response spectra for the ground motions of the four aftershocks (Aftershock 1 to Aftershock 4) measured at four seismic stations (GOK1 to GOK4) in the EW (East-West), NS (North-South) and UD (Up-Down) directions.

slope, and a combination of SV waves and Rayleigh waves amplifies seismic wave at the upper slope (Ohtsuki & Harumi 1983). Therefore, it is possible that seismic waves with large incidence angles have effects on the ground motion amplifications although the slopes are gentle. Given the wave path from epicenters to the study area (West to East), the ground motions in the EW and UD directions could be amplified by Rayleigh waves that were generated by interactions between SV waves with large incidence angles and the ground surface, and those in the NS direction could be amplified by Love waves that were generated by interactions between SH waves and the ground surface.

## 6 CONCLUSIONS

The M5.4 Pohang, South Korea earthquake caused numerous damages including structural damages and geotechnical deformations in spite of the moderate magnitude. We found that serious damages occurred in the northern part of the study area on slopes directed to the main shock epicenter, on plateaus after upslopes, or on ridges, but only few minor damages occurred in the southern district which is on slopes in the opposite directions even though geological conditions and epicentral distances are similar. We installed four temporary seismic stations in the study area and recorded ground motions from the four aftershocks. From these aftershock recordings, we observed ground motion amplifications at the northern part relative to the southern part, which is consistent with the observed damage pattern. Given the similar geological/soil conditions between the two parts in the study area (i.e., $V_{S30}$ profiles ranging from 200 to 400 m/s), we conclude that the different extents of damages are attributed to the ground motions amplified due to surface topographic irregularities and the surface waves generated due to large incidence angles.

## ACKNOWLEDGEMENTS

This research was supported by a grant from the project entitled "Development of liquefaction damage prediction visualization system and liquefaction reinforcement method with high efficiency and low cost" which is funded by the Korea Institute of Civil Engineering and Building Technology (KICT) and the Basic Science Research Program through the National Research Foundation of Korea (NRF) funded by the Ministry of education [NRF-2018R1A6A3A01012888].

## REFERENCES

Aki, K. & Larner, K.L. 1970. Surface motion of a layered medium having an irregular interface due to incident plane SH waves. *J. Geophys. Res*. 75: 933–954.

Ashford, S.A. & Sitar, N. 1997. Analysis of topographic amplification of inclined shear waves in a steep coastal bluff. *Bull. Seism. Soc. Am*. 87: 692–700.

Asimaki, D. & Mohammadi, K. 2018. On the complexity of seismic waves trapped in irregular topographies. *Soil Dyn. Earthq. Eng*. 114: 424–437.

Assimaki, D., Gazetas, G. & Kausel, E. 2005. Effects of Local Soil Conditions on the Topographic Aggravation of Seismic Motion: Parametric Investigation and Recorded Field Evidence from the 1999 Athens Earthquake. *Bull. Seism. Soc. Am*. 95: 1059–1089.

Assimaki, D., Kausel, E. & Gazetas, G. 2005. Soil-Dependent Topographic Effects: A Case Study from the 1999 Athens Earthquake. *Earthq. Spectra* 21: 929–966.

Boore, D.M. 1972. A note on the effect of simple topography on seismic SH waves. *Bull. Seism. Soc. Am*. 62: 275–284.

Bowden, D.C. & Tsai, V.C. 2017. Earthquake ground motion amplification for surface waves. *Geophys. Res. Lett*. 44: 121–127.

Davis, L.L. & West, L.R. 1973. Observed effects of topography on ground motion. *Bull. Seism. Soc. Am*. 63: 283–298.

Geological Survey of Korea 1964. Explanatory Text of the Geological Map of Pohang Sheet (SHEET 7022-II) Scale 1:50,000. Daejeon, South Korea.

Hashash, Y.M.A., Musgrove, M.I., Harmon, J.A., Groholski, D.R., Phillips, C.A. & Park, D. 2016. DEEPSOIL 6.1, User Manual.

Hough, S.E., Altidor, J.R., Anglade, D., Given, D., Janvier, M.G., Maharrey, J.Z., Meremonte, M., Mildor, B.S.-L., Prepetit, C. & Yong, A. 2010. Localized damage caused by topographic amplification during the 2010 M 7.0 Haiti earthquake. *Nat. Geosci*. 3: 778–782.

Hwang, I.G., Chough, S.K., Hong, S.W. & Choe, M.Y. 1995. Controls and evolution of fan delta systems in the Miocene Pohang Basin, SE Korea. *Sedimentary Geology* 98: 147–179.

Kang, S., Kim, B., Bae, S., Lee, H. & Kim, M. 2019. Earthquake-Induced Ground Deformations in the Low-seismicity Region: A case of the 2017 M5.4 Pohang, South Korea, Earthquake. *Earthq. Spectra*: (accepted).

Korea Meteorological Administration 2017. Detailed analysis of 15 Nov Pohang earthquake (Press release). available at http://www.kma.go.kr/notify/press/kma_list.jsp?bid=press&mode=view&num=1193456&page=3&field=&text= (last accessed 5 Nov 2018)

Kovacs, W.D., Seed, H.B. & Idriss, I.M. 1971. Studies of seismic response of clay banks. *J. Soil Mech. Found. Div. ASCE* 97: 441–455.

National Earthquake Comprehensive Information System (NECIS) 2018. available at http://necis.kma.go.kr/ (last accessed 7 November 2018)

Ohtsuki, A. & Harumi, K. 1983. Effect of topography and subsurface inhomogeneities on seismic SV waves. *Earthq. Eng. Struct. Dyn*. 11: 441–462.

Rai, M., Rodriguez-Marek, A. & Asimaki, D. 2016. Topographic proxies from 2-D numerical analyses. *Bulletin of Earthquake Engineering* 14: 2959–2975.

Savage, W.Z. 2004. An Exact Solution for Effects of Topography on Free Rayleigh Waves. *Bull. Seism. Soc. Am*. 94: 1706–1727.

Stamatopoulos, C.A., Bassanou, M., Brennan, A.J. & Madabhushi, G. 2007. Mitigation of the seismic motion near the edge of cliff-type topographies. *Soil Dyn. Earthq. Eng*. 27: 1082–1100.

Tsai, V.C., Bowden, D.C. & Kanamori, H. 2017. Explaining extreme ground motion in Osaka basin during the 2011 Tohoku earthquake. *Geophys. Res. Lett*. 44: 7239–7244.

Wood, C.M. & Cox, B.R. 2016. Comparison of Field Data Processing Methods for the Evaluation of Topographic Effects. *Earthq. Spectra* 32: 2127–2147.